Chloride intracellular channel (CLIC) protein function in S1P-induced Rac1 activation requires membrane localization of the C-terminus, but not thiol-transferase nor ion channel activities.

1 **De Yu Mao[1], Jordan J. Jesse[1,2], Daniel D. Shaye[1, 3]* , Jan Kitajewski[1, 4] ***

2 University of Illinois at Chicago [1]Department of Physiology and Biophysics, [2]Graduate Education in
3 Biomedical Sciences program, [3]Center for Cardiovascular Research, and [4]University of Illinois Cancer
4 Center. 1853 W Polk St. Room 522 (MC 512), Chicago IL 60612.

5 **** Co-senior and co-corresponding authors:** shaye@uic.edu, kitaj@uic.edu.

6 **Running title:** The C-termini of CLIC1 and CLIC4 promote Rac1 activation in response to S1P

7 **Keywords:** CLIC1, CLIC4, RhoA, Rac1, sphingosine-1-phosphate, S1P Receptor, endothelium.

8

9 **Abstract**

10 We have established a novel and evolutionarily-conserved function for chloride intracellular channel

11 proteins (CLICs) in regulating Rho/Rac GTPases downstream of G protein-coupled receptors

12 (GPCRs). Endothelial CLIC1 and CLIC4 are rapidly and transiently re-localized from the cytoplasm

13 to the plasma membrane in response to the GPCR ligand sphingosine-1-phosphate (S1P), and both

14 CLICs are required to activate Rac1 in response to S1P, but how they perform this function remains

15 unknown. Biochemical studies suggest that CLICs act as non-specific ion channels and/or as

16 glutathione-S-transferases, dependent on N-terminal features, *in vitro.* Here we investigate CLIC

17 functional domains and membrane localization requirements for their function in S1P-mediated Rac1

18 signaling. Structure-function analyses of CLIC function in endothelial cells demonstrate that CLIC1

19 and CLIC4-specific functions reside at their C-termini, and that the CLIC4 N-terminus encodes

20 determinants required for S1P-induced re-localization to the plasma membrane but is dispensable for

21 S1P-induced Rac1 activation when the C-terminus is localized to the plasma membrane via a

22 heterologous signal. Our results demonstrate that the postulated ion channel and thiol-transferase

23 activities of CLICs are not required for Rac1 activation and suggests that sequences in the CLIC C-

24 termini are critical for this function. Given the importance of S1P signaling in vascular biology and

25 disease, our work establishes a platform to further our understanding of the membrane-localized

26 proteins required to link GPCR activity to Rho/Rac regulation.

27 **Introduction**

28   Chloride intracellular channels (CLIC) are a family of evolutionarily conserved proteins whose

29   physiological and molecular functions remained poorly defined until recent work from us, and others,

30   demonstrated a role for them in G protein-coupled receptor (GPCR) and Rho-family GTPase signaling

31   that is conserved from *C. elegans* to humans (Tavasoli et al., 2016; Mao et al., 2021; Arena et al., 2022;

32   Kleinjan et al., 2023). CLICs can exist as nuclear, cytoplasmic, and/or membrane-associated forms,

33   and different extracellular signals or physiological conditions can promote re-localization between

34   these different cellular compartments (Novarino et al., 2004; Ponsioen et al., 2009; Malik et al., 2010;

35   Gurski et al., 2015; Lecat et al., 2015; Carlini et al., 2020; Mao et al., 2021; Kleinjan et al., 2023).

36   Although some CLICs transiently, or constitutively, reside at the plasma membrane, chloride channel

37   activity for these proteins under physiological conditions has been challenging to establish (reviewed

38   in Argenzio and Moolenaar, 2016), raising the question as to whether their postulated ion channel

39   activity is required for downstream functions. Moreover, the crystal structure of invertebrate and

40   human CLICs (Littler et al., 2004; Littler et al., 2005; Cromer et al., 2007; Littler et al., 2008) revealed

41   that these proteins resemble the omega family of glutathione-S-transferases (Ω-GSTs), and purified

42   CLIC1 and CLIC4 exhibit GST activity *in vitro* (Al Khamici et al., 2015). However, to date it is not

43   known if the proposed GST and/or ion channel activities are relevant to CLIC function in GPCR and

44   Rho-family GTPase signaling.

45   Out of six mammalian paralogs, CLIC1 and CLIC4 are expressed in the endothelium (Tung et

46   al., 2009; Tung and Kitajewski, 2010; Mao et al., 2021), and we previously used human umbilical vein

47   endothelial cells (HUVEC) to establish that CLIC1 and CLIC4 are required for cell viability, migration,

48   and angiogenic behaviors (Tung et al., 2009; Tung and Kitajewski, 2010). We also found that activation

49   of the sphingosine-1-phosphate (S1P) and thrombin GPCR pathways induces transient re-localization

50   of CLIC1 and/or CLIC4 to the plasma membrane, and that CLIC1 and CLIC4 function in distinct

51   GPCR cascades to regulate RhoA and/or Rac1 activation (Mao et al., 2021; Kleinjan et al., 2023).

52   Specifically CLIC1 and CLIC4 function in sphingosine-1-phosphate receptor (S1PR) signaling (Mao

53   et al., 2021) *in vitro*, while CLIC4 functions in the thrombin/protease activated receptor (PAR) pathway

54   not only in cultured endothelial cells, but also *in vivo* (Kleinjan et al., 2023). Here evaluate CLIC

55   function in S1P signaling (summarized in Fig. 1A). S1P binding to S1PR1 activates its coupled $G\alpha$

56   subunit, $G\alpha_i$, which in turn activates Rac1, promoting cell spreading, migration, and endothelial barrier

57   enhancement (Sugimoto et al., 2003; Kono et al., 2004; Reinhard et al., 2017), while S1P binding to

58   S1PR2 and S1PR3 activates RhoA, via $G\alpha_{12/13}$, leading to stress-fiber formation, cell contraction and

59   endothelial barrier disruption (Lee et al., 1999; Miura et al., 2000; Blaho and Hla, 2011; Reinhard et

60   al., 2017). We found that S1P induces a rapid and transient re-localization of both CLIC1 and CLIC4

61   from the cytoplasm to the plasma membrane, and that both CLICs are required for S1P-induced Rac1

62   activation, while only CLIC1 is required for RhoA activation (Mao et al., 2021). Notably, CLIC1 and

63   CLIC4 have non-overlapping functions in S1P-induced RhoA and Rac1 activation, as CLIC1

64   overexpression does not rescue the Rac1 activation defect caused by RNAi-mediated *CLIC4*

65   knockdown, nor does CLIC4 overexpression rescue the Rac1 or RhoA activation defects caused by

66   *CLIC1* knockdown (Mao et al., 2021).

67   Function of the *C. elegans* CLIC ortholog EXC-4 is strictly dependent on membrane

68   localization (Berry et al., 2003; Berry and Hobert, 2006), and S1P induces rapid re-localization of

69   CLIC1 and CLIC4 to the plasma membrane (Mao et al., 2021). The goals of this study are to determine

70   which domain(s) mediate CLIC1 and CLIC4-specific functions in GPCR-induced Rho-family GTPase

71   activation, and if these domains function at the plasma membrane. We demonstrate that the CLIC1 and

72   CLIC4 C-termini define their specific functions in Rac1 activation in response to S1P in endothelial

73   cells. Moreover, we show that the CLIC4 N-terminus is required for S1P-induced re-localization from

74   the cytoplasm to the plasma membrane, consistent with the previously-described function for an N-

75   terminal putative transmembrane domain (PTMD) in membrane accumulation of EXC-4 in *C. elegans*

76   (Berry et al., 2003; Berry and Hobert, 2006). Finally, we show that the CLIC4 N-terminus is

77   dispensable for S1P-induced Rac1 activation and endothelial barrier function when replaced with a

78   heterologous plasma membrane-targeting motif; the myristylation (myr) signal of the kinase Lck

79   (Bijlmakers et al., 1997; Zlatkine et al., 1997). Given that the myr signal does not possess GST activity

80   or form ion channels, our results demonstrate that these postulated CLIC activities are dispensable for

81   their function in GPCR-induced Rho-family GTPase activation. Our results support a model where

82   CLIC C-termini function at the membrane to facilitate GPCR regulation of Rho-family GTPases.

83

84   **Results**

85   **CLIC1 and CLIC4 functions in S1P-induced Rac1 activation are specified by their C-termini.**

86   Structure-function studies in *C. elegans* showed that the first 66 N-terminal amino-acids of

87   EXC-4 are necessary and sufficient for plasma membrane localization (Berry et al., 2003; Berry and

88   Hobert, 2006), defining a putative transmembrane domain (PTMD) that encompasses two ß-sheets

89   flanking an α-helix; structural elements that are conserved in CLIC1 and CLIC4 (Fig. 1B. Harrop et

90   al., 2001; Littler et al., 2005; Littler et al., 2008). The PTMD resides within the "thioredoxin fold" (Fig.

91   1B), which encodes the thiol-transferase activity of Ω-GSTs that is dependent on a catalytic cysteine

92   found at the start of the first alpha helix (α1, red in Fig. 1B, C). The overlap between the PTMD and

93   the thioredoxin fold, combined with biochemical and biophysical studies (Littler et al., 2004; Singh

94   and Ashley, 2006; Goodchild et al., 2009; Goodchild et al., 2010; Al Khamici et al., 2015; Hare et al.,

95   2016), has led to a model where redox conditions and GST-like activity of CLICs induces a

96   conformational change that exposes the PTMD, resulting in plasma membrane insertion of the N-

97   terminus of CLIC proteins. However, the cysteine required for GST activity is absent from *C. elegans*

98   EXC-4 (Fig. 1B), which constitutively localizes to the plasma membrane (Berry et al., 2003) and

99   which we showed also regulates Rho/Rac signaling in *C. elegans* (Arena et al., 2022). Therefore,

100 questions remain as to whether the postulated GST or channel activities are indeed required for EXC-

101 4/CLIC function in Rho-family signaling,

102   We previously established functional assays for CLIC1 and CLIC4 by infecting HUVEC with

103 lentivirus expressing short-hairpin RNA to reduce *CLIC1* or *CLIC4* expression (hereafter $CLIC1^{KD}$ or

104 $CLIC4^{KD}$) and co-infecting with lentivirus expressing N-terminally HA-tagged CLIC1 or CLIC4 (see

105 Methods and Fig. 1C). Using this approach, we established that HA-CLIC1 rescued phenotypes caused

106 by $CLIC1^{KD}$ but not $CLIC4^{KD}$, while HA-CLIC4 rescued $CLIC1^{KD}$ but not $CLIC4^{KD}$ (Mao et al., 2021),

107 indicating that there is specificity to CLIC function in S1P signaling, and that both CLICs are required,

108 non-redundantly, to facilitate the S1PR1-Gαi branch of the pathway and to activate Rac1.

109   Because the EXC-4 N-terminus promotes membrane accumulation but does not by itself rescue

110 *C. elegans exc-4* null mutants (Berry et al., 2003; Berry and Hobert, 2006), we hypothesized that the

111 CLIC1 and CLIC4 N-termini also primarily mediate localization, while CLIC-specific signaling

112 functions are encoded by their C-termini. To test this, we created HA-tagged chimeras (see Methods,

113 and Figs. 1C, 2A), where the N-terminus of CLIC1 was fused to the C-terminus of CLIC4 (C1-C4),

114 and vice-versa (C4-C1), and assessed their expression in HUVEC, finding that the chimeras are well-

115 expressed in these cells (Fig. 2A). We next tested the ability of these chimeras to rescue $CLIC1^{KD}$ or

116 $CLIC4^{KD}$ phenotypes in HUVEC, and found that full-length CLIC1 and C4-C1, but not the C1-C4

117 chimera, rescued $CLIC1^{KD}$ defects in S1P-induced Rac1 activation and endothelial barrier

118 enhancement measured via trans-endothelial electrical resistance, or TEER (Fig. 2B, D). Conversely,

119 $CLIC4^{KD}$ defects were significantly rescued by full-length CLIC4 and by C1-C4, but not by the C4-C1

120 chimera (Fig. 2C, E). These results demonstrate that the CLIC1 and CLIC4 C-termini provide

121 specificity to CLIC function in endothelial S1P-induced Rac1 activation.

122

123 **The PTMD is necessary for S1P-induced CLIC4 membrane re-localization and Rac1 activation.**

124   To further probe the function of the CLIC N- and C-termini, we generated a truncated CLIC4

125   lacking the PTMD (hereafter (ΔPTMD)CLIC4. See Figs. 1B, 3A.) and expressed this truncated protein

126   in HUVEC. We assessed expression via western blotting, and although we detected a band of the

127   expected size, expression levels were consistently low for this truncation (Fig. 3A). We found that

128   (ΔPTMD)CLIC4, like full-length protein, localized to the cytoplasm and nucleus in the absence of S1P

129   (Fig. 3B). However, and unlike full-length CLIC4, this localization was not affected by S1P treatment

130   (Fig. 3B). Therefore, the CLIC4 PTMD is necessary for re-localization from the cytoplasm to the

131   plasma membrane in response to S1P. We next assessed (ΔPTMD)CLIC4 function and found that this

132   protein did not rescue the Rac1 activation (Fig. 3C) or TEER defects (Fig. 3D) caused by *CLIC4^{KD}*.

133   This lack of function suggests that either the lower levels of (ΔPTMD)CLIC4 expression precludes

134   efficient rescue, or that PTMD-mediated re-localization of CLIC4 to the plasma membrane is required

135   for its function in S1P-induced Rac1 activation.

136

137   **A membrane-localized form of the CLIC4 C-terminus functions in S1P-induced Rac1 activation**

138   We sought to determine if the prime function of the CLIC4 N-terminus is to facilitate plasma

139   membrane localization, and, based upon the finding that the C-terminus of CLICs confer signaling

140   specificity (Fig. 2), we also posited that the C-terminus may be the domain responsible for CLIC4-

141   mediated Rac1 activation. To address these questions, we used a heterologous membrane-localization

142   signal, the myristylation (myr) signal of the kinase Lck (Bijlmakers et al., 1997; Zlatkine et al., 1997),

143   to induce constitutive membrane localization of ectopically expressed CLIC4. We generated two new

144   constructs with myr signal appended to the N-terminal HA-tag: a full length myr-CLIC4, to assess

145   effects of the myr signal on full-length CLIC4 expression and function, and a truncated myr-

146   (ΔPTMD)CLIC4, and assessed expression of these constructs in HUVEC via western blotting, finding

147   single bands of the expected size, with the truncated form again consistently showing lower expression

148   than the full-length protein (Fig. 4A). Notably, both myr-CLIC4 and myr-(ΔPTMD)CLIC4 displayed

149   constitutive membrane accumulation in the absence of S1P (Fig. 4B), indicating that, as expected, the

150   myr signal confers constitutive membrane accumulation of both CLIC4 constructs. Importantly, both

151   myr-CLIC4 and myr-(ΔPTMD)CLIC4 rescued the Rac1 activation (Fig. 4C) and TEER defects (Fig.

152   4D) caused by *CLIC4^{KD}*. Thus, we conclude that the myr signal does not interfere with CLIC4 function.

153   The finding that myr-(ΔPTMD)CLIC4 rescues *CLIC4^{KD}*, leads us to conclude that the C-terminal

154   domain carries the effector function of CLIC4 downstream of S1PR. Finally, as the N-terminus,

155   contains sequences necessary for GST-like and ion channel activities, our findings establish that GST

156   or ion channel activity is not necessary for CLIC4 function in S1P-induced Rac1 activation.

5

Discussion

CLICs have emerged as conserved players in Rho-family GTPase signaling in contexts as diverse as the *C. elegans* excretory canal (Arena et al., 2022), mouse kidney podocytes (Tavasoli et al., 2016), human endothelial cells and mouse vasculature (Mao et al., 2021; Kleinjan et al., 2023). The molecular function of CLICs has long-remained mysterious, with structural and biochemical studies suggesting they may function as channel and/or thiol-transferases (reviewed in Argenzio and Moolenaar, 2016). However, questions remained as to the relevance of these postulated CLIC activities for their emerging role in Rho-family GTPase signaling. We addressed this issue by undertaking structure-function studies in human endothelial cells and our results demonstrate that the signaling functions of CLIC1 and CLIC4 reside at their C-termini, while the N-terminus is dispensable for function in GPCR signaling and mainly plays a role in promoting plasma membrane accumulation upon GPCR activation. These results are consistent with findings in *C. elegans*, where it was shown that the PTMD of EXC-4, which lacks a critical cysteine residue required for GST-like activity, is necessary and sufficient for plasma membrane accumulation and is required for EXC-4 function (Berry et al., 2003; Berry and Hobert, 2006). Moreover, we also found that CLIC4 constructs lacking the N-terminal PTMD are expressed at lower levels than full-length protein, even when tethered to the plasma membrane, suggesting that the CLIC4 PTMD may encode determinants that promote stability and/or counteract degradation signals located at the C-terminus.

The activity of Rho-family GTPases is precisely controlled by regulating their localization to the plasma membrane, and by membrane localization of activators (guanine-exchange factors, or RhoGEFs) and inhibitors (GTPase-activating proteins, or RhoGAPs). Therefore, our finding that plasma membrane accumulation of the CLIC4 C-terminus is required for Rac1 activation in response to S1P suggests a model where CLIC C-termini activate Rho-family GTPases either directly or as part of a complex with RhoGEFs and/or RhoGAPs. If CLICs directly activate Rho-family GTPases, we might expect that constitutive recruitment of full-length, or just the C-terminus of, CLIC4 to the plasma membrane could be sufficient to activate Rac1. However, we did not observe activation of Rac1 in cells expressing myr -CLIC4 or myr-(ΔPTMD)CLIC4 in the absence of S1P (Supplemental Fig. S1), indicating that CLICs are necessary, but not sufficient, to activate Rho-family GTPases in response to GPCR ligands. We expect that continued structure-function studies to elucidate C-terminal sequences required for EXC-4/CLIC function, combined with discovery of EXC-4/CLIC-interacting proteins required for function, will reveal the novel and conserved molecular mechanisms by which CLICs regulate Rho-family GTPase activity.

6

Materials and Methods

Primary cells and cell culture

Pooled HUVECs from different donors were either directly isolated from human umbilical cords following established protocols (Jaffe et al., 1973) or purchased (Lonza, Cat# C2519A). HUVEC were grown in EGM-2 Endothelial Cell Growth Media (Lonza), including all supplements provided, on culture dishes coated with rat tail type I collagen (Corning). 293T cells were acquired from the American Type Culture Collection and maintained in high-glucose Dulbecco's modified Eagle's medium (Gibco) with 10% heat-inactivated fetal bovine serum (HI-FBS) and 0.01% penicillin-streptomycin. Unless otherwise noted, cells were cultured under standard conditions in a humidified incubator at $37^{\circ}C$, 5% CO_2.

RNAi-mediated CLIC1 and CLIC4 knockdown constructs

Validated control (scrambled) shRNA, and human CLIC1 and CLIC4 shRNA-expressing lentiviruses, based on the pLKO.1 vector backbone (Moffat et al., 2006), from Sigma-Millipore were as previously-described (Tung et al., 2009; Tung and Kitajewski, 2010; Mao et al., 2021; Kleinjan et al., 2023).

Tagged CLIC1 and CLIC4 constructs

Full-length HA-tagged CLIC1 and CLIC4 plasmids were previously described (Mao et al., 2021), and the derived chimeric and truncated variants used here were made using standard molecular cloning techniques, and DNA sequencing was performed to verify the correct sequence before experiments (details available upon request). All HA-tagged constructs were cloned into the pCCL lentivirus vector (Dull et al., 1998) for delivery and expression in HUVEC

Lentivirus-mediated stable overexpression and/or knockdown in HUVEC

To perform knockdown and/or overexpression in HUVEC, a lentiviral infection system was utilized. For lentiviral gene transfer, 293T cells were transfected using the calcium phosphate approach with the following combination of plasmids: 3μg of pVSVG, 5μg of pMDLg/pRRE, 2.5μg of pRSV-Rev, and 10μg of the overexpression (pCCL-based) and/or knockdown (pLKO.1-based) vectors of interest. Transfected 293T cells were allowed to produce lentivirus and the supernatant was collected 48 hours post transfection. The supernatant collected was passed through a 0.45μm filter and then added onto HUVEC. A single round of infection was performed for 24hrs. The primary cells were allowed to express shRNA or overexpression constructs for at least 48 hours before experiments. A red-flourescent construct (pCCL-RFP) was included in all experiments to assess infection efficiency.

Reagents and Antibodies

Sphignosine-1-phosphate (S1P) was obtained from Enzo Life Sciences (BML-SL140). Antibodies to human CLIC1 (Abcam ab28722, Rabbit, 1:250), human CLIC4 (Novus Biologicals NBP1-85574, Rabbit, 1:250), HA (GenScript A01244, Mouse, 1:500), tubulin (Sigma-Aldrich T6074, 1:5000), and VE-cadherin (Abcam ab33168, Rabbit, 1:250) were used for immunoblotting and immunofluorescence as described below.

Immunoblotting

HUVECs were washed with cold PBS, and lysates were collected with TENT lysis buffer (50mM Tris pH 8.0, 2mM EDTA, 150mM NaCl, and 1% Triton X-100) containing a protease inhibitor cocktail (EMD Chemicals Inc.). Protein lysates were collected by centrifugation at 14000rpm for 10 minutes. Lysates were boiled at $95^{\circ}C$ for 5 minutes with addition of sample buffer containing SDS and β-mercaptoethanol. Protein concentrations were measured using the Bradford protein assay (Bio-Rad Laboratories). Volumes were adjusted to ensure equal amounts of protein loading. SDS-PAGE was

233 performed for 1 hours at 150V, followed by wet transfer of proteins onto a nitrocellulose membrane
234 for 1 hour at 100V. Blocking of the nitrocellulose membrane was with 5% BSA in TBS-Tween solution
235 for 1 hour. Primary antibody incubation was done in 2.5% BSA overnight at 4°C, and secondary
236 antibody incubation was done the next day for 2hr at room temperature. The membrane was developed
237 using Clarity™ Western ECL Substrate (Bio-Rad) and protein bands were observed. Densitometry
238 analysis was performed with GelAnalyzer 19.1 by Istvan Lazar Jr., PhD and Istvan Lazar Sr., PhD,
239 CSc (available at www.gelanalyzer.com).

Immunofluorescence
241 Cells were plated on 8-well collagen-coated chamber slides (Ibidi). 50,000 cells were seeded onto each
242 well overnight. The next day cells were serum starved for 3 hours prior to S1P treatment. 1μM S1P for
243 various times points was used to treat HUVECs, followed by fixation with 4% PFA for 10 minutes.
244 Cells were then washed 3 times with PBS and blocked with 3% BSA and 0.1% TritonX-100. Primary
245 antibodies were used at the listed dilutions in blocking solution and incubated overnight at 4°C. Cells
246 were then washed with 1XPBS, 3 times for 5 minutes each and incubated with secondary antibody
247 Alexa Fluor 488 (green) or Alexa Fluor 647 (far-red) at 1:1000 in blocking solution for 2hrs. After
248 washing cells 3 times after secondary antibody incubation, cells were mounted using VectaShield with
249 DAPI (Vector Labs). Slides were imaged using Airyscan confocal microscopy with a Zeiss laser
250 scanning microscope (LSM800). Images analysis was done with ZEN software under the same
251 acquisition setting for among all cell lines in each experiment.

Rac1 G-LISA activation assay
253 Assays were performed using a Rac1 (Cytoskeleton, BK128) G-LISA Activation Assay Kits. HUVECs
254 were serum-starved in EGM-2 with 1% serum overnight and with serum-free EBM-2 for an additional
255 3 hours the following day. The cells were then stimulated with 1 μM S1P for Rac1 activation. Cell
256 lysates were harvested and snap-frozen in liquid nitrogen. The assay was then performed based on the
257 manufacturer's protocol.

Trans-endothelial electrical resistance (TEER) assay
259 An ECIS array plate (Applied Biophysics) containing circular 250μm diameter active electrodes
260 connected in parallel on a common gold pad was coated with rat tail type I collagen (Corning). HUVEC
261 cells were seeded at 50,000 cells per well and allowed to grow overnight. Cells were serum starved
262 (EBM-2, Lonza) for 2 hours, followed by a 30-min baseline resistance stabilization with the Electrical
263 Cell-Substrate Impedance Sensing (ECIS) system (Applied Biophysics, model 1600R). 1μM S1P or
264 BSA vehicle control were administered, and trans-endothelial resistance was monitored at a frequency
265 of 4000Hz with measurements taken at 3-min intervals for 24 hours. Quantifications were performed
266 by area under the curve analysis using GraphPad Prism software.

Statistics
268 All experiments were repeated at least three times, and statistical tests were performed using GraphPad
269 Prism software. Area under the curve averages and standard error of the mean (SEM) were computed
270 using the Gagnon method, which produces a single value, so individual AUC measurments for each
271 replicate are are not determined. Unless otherwise noted, unpaired 2-tailed t tests were used, and P
272 values less than 0.05 were considered statistically significant.

273

274 **Figure Legends**

275 **Fig. 1: CLIC1 and CLIC4 in endothelial S1P signaling, and CLIC sequence and structural**
276 **features relevant to this study.** (**A**) description of shared and unique functions for CLIC1 and CLIC4
277 in endothelial S1P signaling (Mao et al., 2021). (**B**) Protein sequence alignment of *C. elegans* EXC-4,
278 and human CLIC1 and CLIC4 indicating regions of amino-acid identity (dark grey shading) and
279 similarity (light grey shading). Conserved beta sheets (yellow arrows) and alpha helices (pink rounded
280 boxes) determined by crystal structure of these proteins (Littler et al., 2004; Littler et al., 2005; Littler
281 et al., 2008) are shown. The N-terminal putative transmembrane domain (PTMD) and conserved
282 thioredoxin fold are highlighted. Note that the N-terminal cysteine required for thiol-reductases activity
283 (red), and the C-terminal nuclear localization signal (orange) found in human CLIC1 and 4 are not
284 present in *C. elegans* EXC-4, while the *C. elegans* protein has a C-terminal extension with additional
285 alpha helices (α10, α11). (**C**) cartoon representation of HA-tagged full-length CLIC1 and CLIC4
286 constructs. The C-terminal fragments swapped in the chimeric constructs analyzed in Fig. 2 are denoted
287 in blue, and the ΔPTMD CLIC4 truncation analyzed in Figs. 3 and 4 is denoted in purple (the precise
288 protein sequence location for these constructs are shown as blue and purple arrows in panel B).

289 **Fig. 2: CLIC1 and CLIC4-specific functions in S1P signaling are encoded by their C-termini.** (**A**)
290 cartoon representation of the C1-C4 and C4-C1 chimeras, and western blot analysis and quantification
291 (n=4) of their expression in HUVEC (see Methods). (**B**) full-length CLIC1 and the C4-C1 chimera
292 rescue the Rac1 activation defect caused by *CLIC1^{KD}*, as assessed by G-LISA (see Methods). (**C**) full-
293 length CLIC4 and the C1-C4 chimera rescue the Rac1 activation defect caused by *CLIC4^{KD}*, as assessed
294 by G-LISA. In panels (B) and (C) each bar represents the mean of n$\geq$3 replicates, the error bars
295 represent standard deviation (hereafter, SD), and significance between vehicle control (Veh.) and S1P-
296 treated cells was calculated via unpaired t-tests. HUVEC monolayers form a barrier whose strength
297 can be measured via a trans-endothelial electrical resistance (TEER) assay, and stimulation by S1P
298 rapidly, and reversibly, enhances HUVEC barrier function (Garcia et al., 2001). We previously showed
299 that *CLIC1* or *CLIC4* knockdown reduced S1P-induced barrier strengthening (Mao et al., 2021), and
300 here we show that (**D**) full-length CLIC1 and the C4-C1 chimera rescue the barrier defect caused by
301 *CLIC1^{KD}* (see Methods), while (**E**) full-length CLIC4 and the C1-C4 chimera rescue the TEER defect
302 caused by *CLIC4^{KD}*. Each trace represents the mean TEER measurement of n$\geq$3 samples, normalized
303 to the TEER value at time of S1P addition (see Methods). To quantify these results, the area under the
304 curve (AUC) $\pm$ standard error of the mean (SEM) from the time of S1P addition (~30min. after
305 beginning of resistance measurements) until time of maximal recovery to baseline in control (~60 min.
306 after beginning of experiment, ~30 min. after S1P addition) was calculated for each condition (see
307 Methods), and these results are shown in the accompanying bar graphs. Significance was calculated
308 using unpaired 2-tailed t tests.
309

310 **Fig. 3: The N-terminal putative transmembrane domain (PTMD) is required for CLIC4 re-**
311 **localization and Rac1 activation in response to S1P.** (**A**) cartoon representation of the HA-tagged
312 (ΔPTMD)CLIC4 construct, and western blot analysis and quantification (n=3) of its expression in
313 HUVEC (see Methods), as compared to full-length HA-CLIC4. (**B**) Immunofluorescence of full-length
314 HA-tagged CLIC4 (top) and (ΔPTMD)CLIC4, and their localization after treatment with S1P (see
315 Methods). Both constructs showed nuclear and cytoplasmic accumulation prior to S1P treatment.
316 Noticeable accumulation of full-length CLIC4 was observed near the cell cortex (outlined by VE-
317 cadherin) within 5 minutes and remained at 10 and 15 minutes after S1P addition (yellow arrows, top
318 rows). In contrast we did not observe similar re-localization of the (ΔPTMD)CLIC4 construct (bottom
319 rows). Scale bar represents 50μm in all panels. (**C**) the (ΔPTMD)CLIC4 construct does not rescues the
320 Rac1 activation defect caused by *CLIC4^{KD}*, as assessed by G-LISA. Each bar represents the mean of

321 n≥3 replicates, the error bars represent SD, and significance between vehicle control (Veh.) and S1P-
322 treated cells was calculated via unpaired t-tests. (**D**) the (ΔPTMD)CLIC4 construct does not rescue the
323 TEER defect caused by *CLIC4^{KD}*. Each trace represents the mean TEER measurement of n≥3 samples,
324 normalized to the TEER value at time of S1P addition, and quantitative AUC analysis of TEER
325 calculation was carried out as described in Fig. 2D and 2E.

326

327 **Fig. 4: Membrane localized CLIC4 C-terminus is sufficient to promote Rac1 activation in**
328 **response to S1P.** (**A**) cartoon representation of HA-tagged full-length myristylated (myr) CLIC4 and
329 myr-(ΔPTMD)CLIC4, lacking the N-terminal putative transmembrane domain. Western blot analysis
330 and quantification (n=3) of construct expression in HUVEC (see Methods), shows lower expression of
331 myr-(ΔPTMD)CLIC4 as compared to full-length myr-CLIC4. (**B**) Immunofluorescence showing
332 accumulation of HA-tagged full-length CLIC4 (first column), myr-CLIC4 (second column) and myr-
333 (ΔPTMD)CLIC4 (third column) at steady state (no S1P). Note that both myristylated constructs display
334 accumulation at the membrane (yellow arrows), and decreased nuclear accumulation (cyan asterisks)
335 when compared to wildtype full-length CLIC4. Scale bar represents 50µm in all panels. (**C**) both the
336 full-length myr-CLIC4 and the myr-(ΔPTMD)CLIC4 constructs rescue the Rac1 activation defect
337 caused by *CLIC4^{KD}*, as assessed by G-LISA. Each bar represents the mean of n≥3 replicates, the error
338 bars represent SD, and significance between vehicle control (Veh.) and S1P-treated cells was
339 calculated via unpaired t-tests. (**D**) (**C**) both the full-length myr-CLIC4 and the myr-(ΔPTMD)CLIC4
340 constructs rescue the TEER defect caused by *CLIC4^{KD}*. Each trace represents the mean TEER
341 measurement of n≥3 samples, normalized to the TEER value at time of S1P addition, and quantitative
342 AUC analysis of TEER calculation was carried out as described in Fig. 2D and 2E. Dashed lines and
343 bars (Control, *CLIC4^{KD}*, and *CLIC4^{KD}* + CLIC4) are the same data shown in Fig. 3D

344

Conflict of Interest

346 *The authors declare that the research was conducted in the absence of any commercial or financial*
347 *relationships that could be construed as a potential conflict of interest.*

Author Contributions
349 Conceptualization: DYM, JJJ, DDS, JK
350 Data curation: DYM, JJJ
351 Formal analysis: DYM, JJJ, DDS
352 Funding acquisition: JJJ, DDS, JK
353 Investigation: DYM, JJJ
354 Methodology: DYM, JJJ, DDS, JK
355 Project administration: DDS, JK
356 Resources: DDS, JK
357 Supervision: DDS, JK
358 Validation: DYM, JJJ
359 Visualization: DYM, JJJ, DS
360 Writing – original draft: DYM, JK
361 Writing – review & editing: DYM, JJJ, DS, JK

Funding

Acknowledgments

The authors would like to thank Alison Kitajewski for technical support, Matthew J. Kleinjan for help with early stages of this work, and members of the Kitajewski and Shaye laboratories for fruitful discussions during this project.

Supplementary Material

Data Availability Statement

The datasets and reagents generated for this study will be made available by the authors upon request, without undue reservation.

LITERATURE CITED

Al Khamici, H., Brown, L.J., Hossain, K.R., Hudson, A.L., Sinclair-Burton, A.A., Ng, J.P., et al. (2015). Members of the chloride intracellular ion channel protein family demonstrate glutaredoxin-like enzymatic activity. *PLoS One* 10(1)**,** e115699. doi: 10.1371/journal.pone.0115699.

Arena, A.F., Escudero, J., and Shaye, D.D. (2022). A metazoan-specific C-terminal motif in EXC-4 and Galpha-Rho/Rac signaling regulate cell outgrowth during tubulogenesis in C. elegans. *Development* 149(24). doi: 10.1242/dev.200748.

Argenzio, E., and Moolenaar, W.H. (2016). Emerging biological roles of Cl- intracellular channel proteins. *J Cell Sci* 129(22)**,** 4165-4174. doi: 10.1242/jcs.189795.

Berry, K.L., Bulow, H.E., Hall, D.H., and Hobert, O. (2003). A *C. elegans* CLIC-like protein required for intracellular tube formation and maintenance. *Science* 302(5653)**,** 2134-2137. doi: 10.1126/science.1087667.

Berry, K.L., and Hobert, O. (2006). Mapping functional domains of chloride intracellular channel (CLIC) proteins *in vivo*. *J Mol Biol* 359(5)**,** 1316-1333. doi: 10.1016/j.jmb.2006.04.046.

Bijlmakers, M.J., Isobe-Nakamura, M., Ruddock, L.J., and Marsh, M. (1997). Intrinsic signals in the unique domain target p56(lck) to the plasma membrane independently of CD4. *J Cell Biol* 137(5)**,** 1029-1040.

Blaho, V.A., and Hla, T. (2011). Regulation of mammalian physiology, development, and disease by the sphingosine 1-phosphate and lysophosphatidic acid receptors. *Chem Rev* 111(10)**,** 6299-6320. doi: 10.1021/cr200273u.

Carlini, V., Verduci, I., Cianci, F., Cannavale, G., Fenoglio, C., Galimberti, D., et al. (2020). CLIC1 Protein Accumulates in Circulating Monocyte Membrane during Neurodegeneration. *Int J Mol Sci* 21(4). doi: 10.3390/ijms21041484.

Cromer, B.A., Gorman, M.A., Hansen, G., Adams, J.J., Coggan, M., Littler, D.R., et al. (2007). Structure of the Janus protein human CLIC2. *J Mol Biol* 374(3)**,** 719-731. doi: 10.1016/j.jmb.2007.09.041.

Dull, T., Zufferey, R., Kelly, M., Mandel, R.J., Nguyen, M., Trono, D., et al. (1998). A third-generation lentivirus vector with a conditional packaging system. *J Virol* 72(11)**,** 8463-8471. doi: 10.1128/JVI.72.11.8463-8471.1998.

Garcia, J.G., Liu, F., Verin, A.D., Birukova, A., Dechert, M.A., Gerthoffer, W.T., et al. (2001). Sphingosine 1-phosphate promotes endothelial cell barrier integrity by Edg-dependent cytoskeletal rearrangement. *J Clin Invest* 108(5)**,** 689-701. doi: 10.1172/JCI12450.

Goodchild, S.C., Howell, M.W., Cordina, N.M., Littler, D.R., Breit, S.N., Curmi, P.M., et al. (2009). Oxidation promotes insertion of the CLIC1 chloride intracellular channel into the membrane. *Eur Biophys J* 39(1)**,** 129-138. doi: 10.1007/s00249-009-0450-0.

Goodchild, S.C., Howell, M.W., Littler, D.R., Mandyam, R.A., Sale, K.L., Mazzanti, M., et al. (2010). Metamorphic response of the CLIC1 chloride intracellular ion channel protein upon membrane interaction. *Biochemistry* 49(25)**,** 5278-5289. doi: 10.1021/bi100111c.

414   Gurski, L.A., Knowles, L.M., Basse, P.H., Maranchie, J.K., Watkins, S.C., and Pilch, J. (2015).
415   Relocation of CLIC1 promotes tumor cell invasion and colonization of fibrin. *Mol Cancer*
416   *Res* 13(2)**,** 273-280. doi: 10.1158/1541-7786.MCR-14-0249.

417   Hare, J.E., Goodchild, S.C., Breit, S.N., Curmi, P.M., and Brown, L.J. (2016). Interaction of Human
418   Chloride Intracellular Channel Protein 1 (CLIC1) with Lipid Bilayers: A Fluorescence Study.
419   *Biochemistry* 55(27)**,** 3825-3833. doi: 10.1021/acs.biochem.6b00080.

420   Harrop, S.J., DeMaere, M.Z., Fairlie, W.D., Reztsova, T., Valenzuela, S.M., Mazzanti, M., et al.
421   (2001). Crystal structure of a soluble form of the intracellular chloride ion channel CLIC1
422   (NCC27) at 1.4-A resolution. *J Biol Chem* 276(48)**,** 44993-45000. doi:
423   10.1074/jbc.M107804200.

424   Jaffe, E.A., Nachman, R.L., Becker, C.G., and Minick, C.R. (1973). Culture of human endothelial
425   cells derived from umbilical veins. Identification by morphologic and immunologic criteria. *J*
426   *Clin Invest* 52(11)**,** 2745-2756. doi: 10.1172/JCI107470.

427   Kleinjan, M.L., Mao, Y., Naiche, L.A., Joshi, J.C., Gupta, A., Jesse, J.J., et al. (2023). CLIC4
428   Regulates Endothelial Barrier Control by Mediating PAR1 Signaling via RhoA. *Arterioscler*
429   *Thromb Vasc Biol* 43(8)**,** 1441-1454. doi: 10.1161/ATVBAHA.123.319206.

430   Kono, M., Mi, Y., Liu, Y., Sasaki, T., Allende, M.L., Wu, Y.P., et al. (2004). The sphingosine-1-
431   phosphate receptors S1P1, S1P2, and S1P3 function coordinately during embryonic
432   angiogenesis. *J Biol Chem* 279(28)**,** 29367-29373. doi: 10.1074/jbc.M403937200.

433   Lecat, S., Matthes, H.W., Pepperkok, R., Simpson, J.C., and Galzi, J.L. (2015). A Fluorescent Live
434   Imaging Screening Assay Based on Translocation Criteria Identifies Novel Cytoplasmic
435   Proteins Implicated in G Protein-coupled Receptor Signaling Pathways. *Mol Cell Proteomics*
436   14(5)**,** 1385-1399. doi: 10.1074/mcp.M114.046698.

437   Lee, M.J., Thangada, S., Claffey, K.P., Ancellin, N., Liu, C.H., Kluk, M., et al. (1999). Vascular
438   endothelial cell adherens junction assembly and morphogenesis induced by sphingosine-1-
439   phosphate. *Cell* 99(3)**,** 301-312. doi: 10.1016/s0092-8674(00)81661-x.

440   Littler, D.R., Assaad, N.N., Harrop, S.J., Brown, L.J., Pankhurst, G.J., Luciani, P., et al. (2005).
441   Crystal structure of the soluble form of the redox-regulated chloride ion channel protein
442   CLIC4. *FEBS J* 272(19)**,** 4996-5007. doi: 10.1111/j.1742-4658.2005.04909.x.
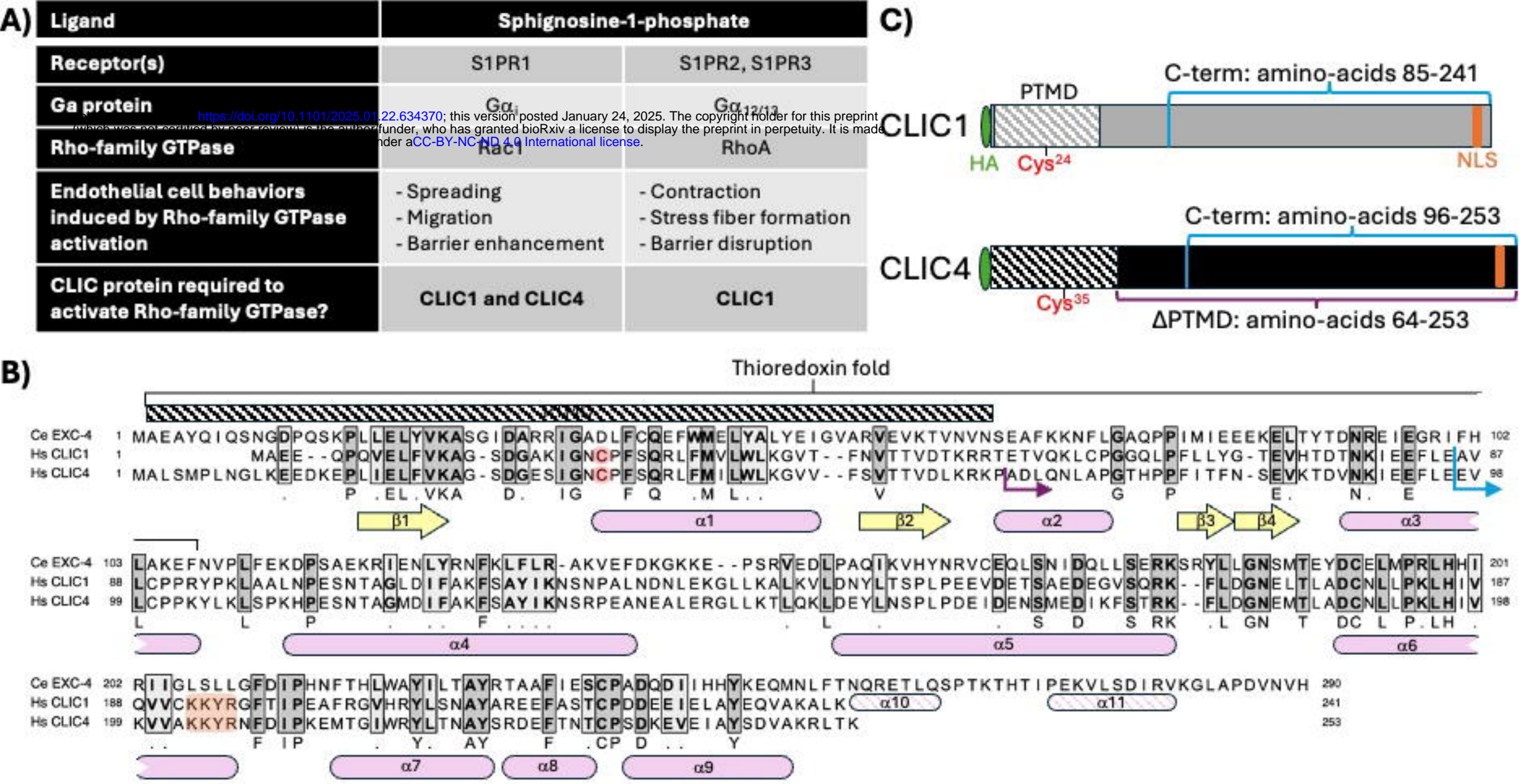
443   Littler, D.R., Harrop, S.J., Brown, L.J., Pankhurst, G.J., Mynott, A.V., Luciani, P., et al. (2008).
444   Comparison of vertebrate and invertebrate CLIC proteins: the crystal structures of
445   *Caenorhabditis elegans* EXC-4 and *Drosophila melanogaster* DmCLIC. *Proteins* 71(1)**,** 364-
446   378. doi: 10.1002/prot.21704.

447   Littler, D.R., Harrop, S.J., Fairlie, W.D., Brown, L.J., Pankhurst, G.J., Pankhurst, S., et al. (2004).
448   The intracellular chloride ion channel protein CLIC1 undergoes a redox-controlled structural
449   transition. *J Biol Chem* 279(10)**,** 9298-9305. doi: 10.1074/jbc.M308444200.

450   Malik, M., Shukla, A., Amin, P., Niedelman, W., Lee, J., Jividen, K., et al. (2010). S-Nitrosylation
451   Regulates Nuclear Translocation of Chloride Intracellular Channel Protein CLIC4. *Journal of*
452   *Biological Chemistry* 285(31)**,** 23818-23828. doi: 10.1074/jbc.M109.091611.

453   Mao, D.Y., Kleinjan, M.L., Jilishitz, I., Swaminathan, B., Obinata, H., Komarova, Y.A., et al. (2021).
454   CLIC1 and CLIC4 mediate endothelial S1P receptor signaling to facilitate Rac1 and RhoA
455   activity and function. *Science Signaling* 14(679)**,** eabc0425. doi: 10.1126/scisignal.abc0425.

13

456   Miura, Y., Yatomi, Y., Rile, G., Ohmori, T., Satoh, K., and Ozaki, Y. (2000). Rho-mediated
457   phosphorylation of focal adhesion kinase and myosin light chain in human endothelial cells
458   stimulated with sphingosine 1-phosphate, a bioactive lysophospholipid released from
459   activated platelets. *J Biochem* 127(5)**,** 909-914. doi: 10.1093/oxfordjournals.jbchem.a022686.

460   Moffat, J., Grueneberg, D.A., Yang, X., Kim, S.Y., Kloepfer, A.M., Hinkle, G., et al. (2006). A
461   lentiviral RNAi library for human and mouse genes applied to an arrayed viral high-content
462   screen. *Cell* 124(6)**,** 1283-1298. doi: 10.1016/j.cell.2006.01.040.

463   Novarino, G., Fabrizi, C., Tonini, R., Denti, M.A., Malchiodi-Albedi, F., Lauro, G.M., et al. (2004).
464   Involvement of the intracellular ion channel CLIC1 in microglia-mediated beta-amyloid-
465   induced neurotoxicity. *J Neurosci* 24(23)**,** 5322-5330. doi: 10.1523/JNEUROSCI.1170-
466   04.2004.

467   Ponsioen, B., van Zeijl, L., Langeslag, M., Berryman, M., Littler, D., Jalink, K., et al. (2009).
468   Spatiotemporal regulation of chloride intracellular channel protein CLIC4 by RhoA. *Mol Biol
469   Cell* 20(22)**,** 4664-4672. doi: 10.1091/mbc.E09-06-0529.

470   Reinhard, N.R., Mastop, M., Yin, T., Wu, Y., Bosma, E.K., Gadella, T.W.J., Jr., et al. (2017). The
471   balance between Gαi-Cdc42/Rac and Gα12/13-RhoA pathways determines endothelial barrier
472   regulation by sphingosine-1-phosphate. *Mol Biol Cell* 28(23)**,** 3371-3382. doi:
473   10.1091/mbc.E17-03-0136.

474   Singh, H., and Ashley, R.H. (2006). Redox regulation of CLIC1 by cysteine residues associated with
475   the putative channel pore. *Biophys J* 90(5)**,** 1628-1638. doi: 10.1529/biophysj.105.072678.

476   Sugimoto, N., Takuwa, N., Okamoto, H., Sakurada, S., and Takuwa, Y. (2003). Inhibitory and
477   stimulatory regulation of Rac and cell motility by the G12/13-Rho and Gi pathways
478   integrated downstream of a single G protein-coupled sphingosine-1-phosphate receptor
479   isoform. *Mol Cell Biol* 23(5)**,** 1534-1545. doi: 10.1128/mcb.23.5.1534-1545.2003.

480   Tavasoli, M., Li, L., Al-Momany, A., Zhu, L.F., Adam, B.A., Wang, Z., et al. (2016). The chloride
481   intracellular channel 5A stimulates podocyte Rac1, protecting against hypertension-induced
482   glomerular injury. *Kidney Int* 89(4)**,** 833-847. doi: 10.1016/j.kint.2016.01.001.

483   Tung, J.J., Hobert, O., Berryman, M., and Kitajewski, J. (2009). Chloride intracellular channel 4 is
484   involved in endothelial proliferation and morphogenesis *in vitro*. *Angiogenesis* 12(3)**,** 209-
485   220. doi: 10.1007/s10456-009-9139-3.

486   Tung, J.J., and Kitajewski, J. (2010). Chloride intracellular channel 1 functions in endothelial cell
487   growth and migration. *J Angiogenes Res* 2**,** 23. doi: 10.1186/2040-2384-2-23.

488   Zlatkine, P., Mehul, B., and Magee, A.I. (1997). Retargeting of cytosolic proteins to the plasma
489   membrane by the Lck protein tyrosine kinase dual acylation motif. *J Cell Sci* 110 (Pt 5)**,** 673-
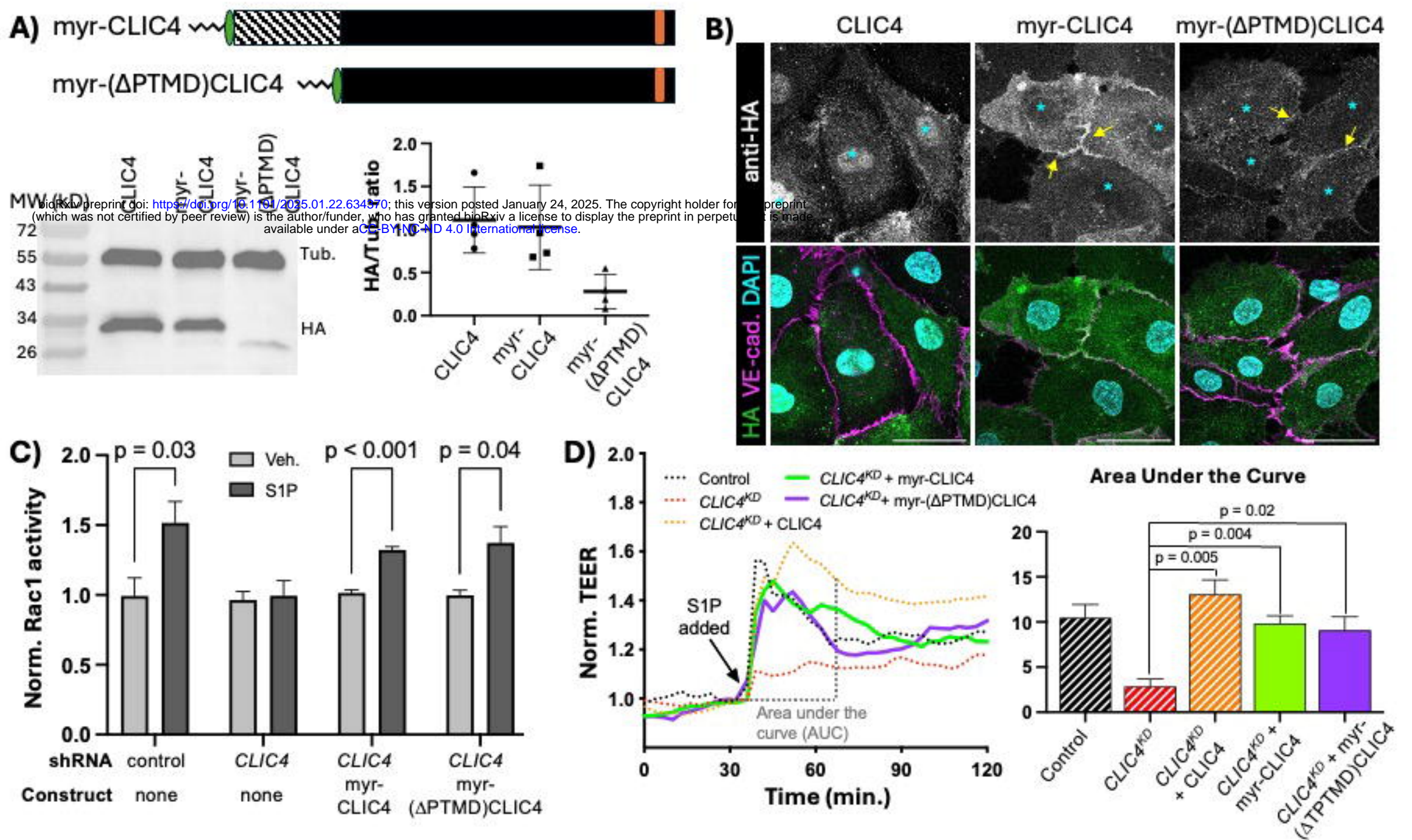490   679.

491

Mao, et al., Figure 1

Mao, et al., Figure 2

A) (ΔPTMD)CLIC4

CLIC4(64-253)

B) Time after S1P addition
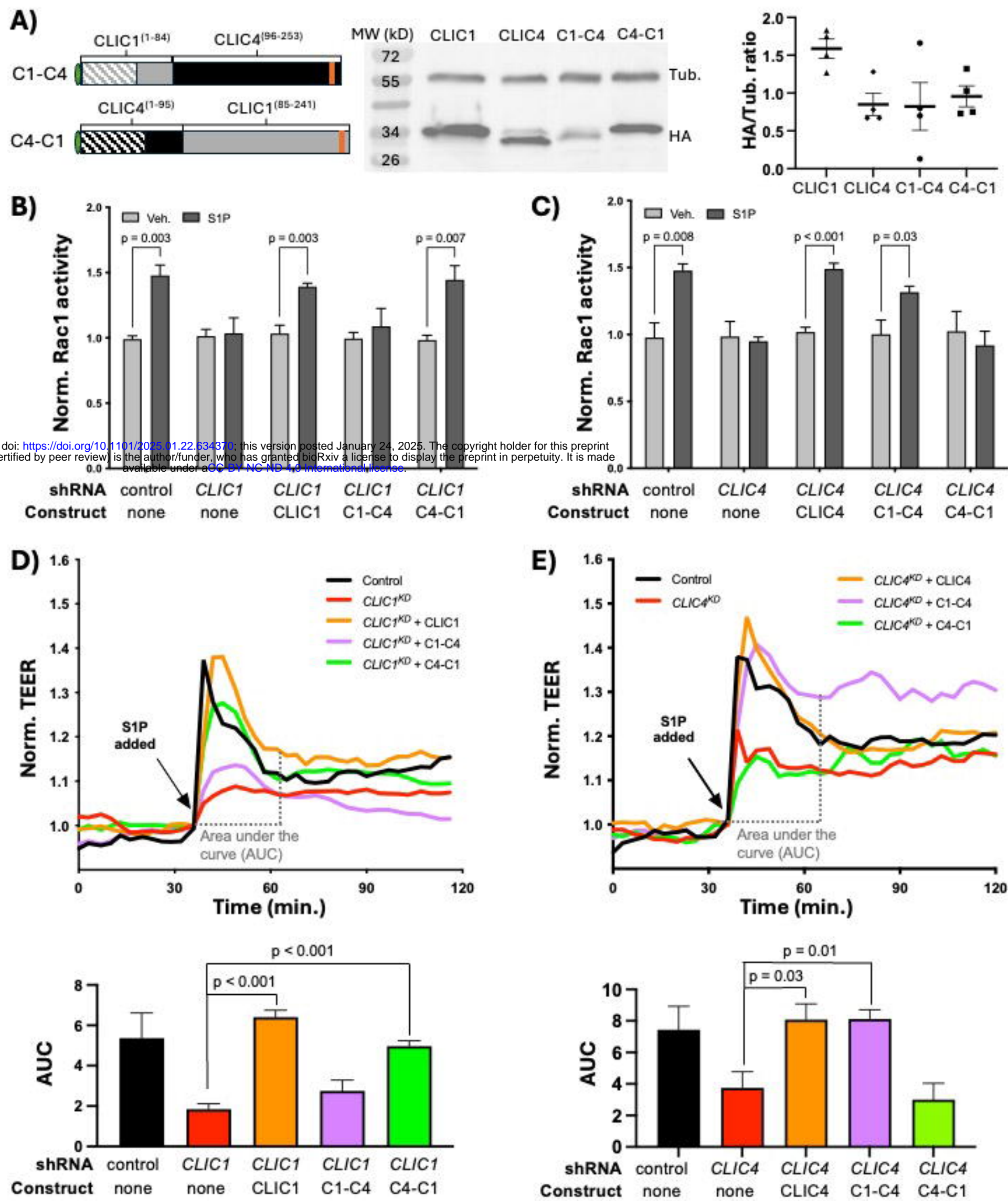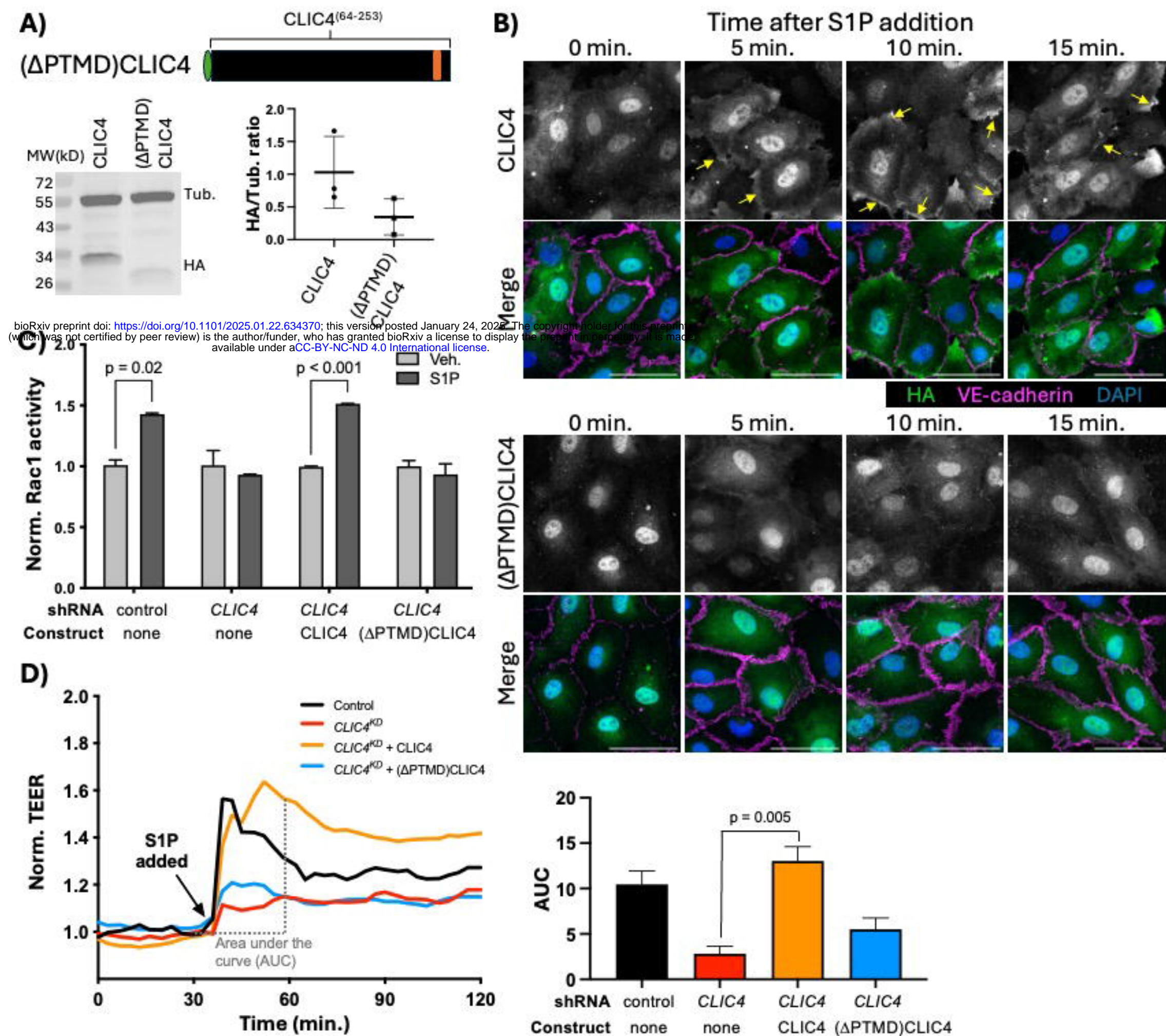
Mao, et al., Figure 3

Mao, et al., Figure 4